



Computing the electronic circular dichroism spectrum of DNA quadruple helices of different topology: A critical test for a generalized excitonic model based on a fragment diabatization

Haritha Asha¹ | James A. Green²  | Luciana Esposito¹ | Fabrizio Santoro³  | Roberto Improta¹

¹Istituto di Biostrutture e Bioimmagini, CNR, Napoli, Italy

²Institut für Physikalische Theoretische Chemie, Goethe-Universität Frankfurt am Main, Frankfurt am Main, Germany

³Istituto di Chimica dei Composti Organometallici (ICCOM-CNR), Area della Ricerca del CNR, Pisa, Italy

Correspondence

Fabrizio Santoro, Istituto di Chimica dei Composti Organometallici (ICCOM-CNR), Area della Ricerca del CNR, Via Moruzzi 1, I-56124 Pisa, Italy.
Email: fabrizio.santoro@iccom.cnr.it

Roberto Improta, Istituto di Biostrutture e Bioimmagini del CNR, Via De Amicis 95, I-80145 Napoli, Italy.
Email: roberto.improta@cnr.it

Funding information

Consiglio Nazionale delle Ricerche; ICSC - Centro Nazionale di Ricerca in High Performance Computing, Big Data and Quantum Computing; CN3 - National Center for Gene Therapy and Drugs based on RNA technology; NextGenerationEU

Abstract

In this study, we exploit a recently developed fragment diabatization-based excitonic model, FrDEX, to simulate the electronic circular dichroism (ECD) spectra of three guanine-rich DNA sequences arranged in guanine quadruple helices with different topologies: thrombin binding aptamer (antiparallel), c-Myc promoter (parallel), and human telomeric sequence (3+1 hybrid). Starting from time-dependent density functional theory (TD-DFT) calculations with the M052X functional, we apply our protocol to parameterize the FrDEX Hamiltonian, which accounts for electron density overlap and includes both the coupling with charge transfer transitions and the effect of the surrounding bases on the local excitation of each chromophore. The TD-DFT/M052X spectral shapes are in good agreement with the experimental ones, the main source of discrepancy being related to the intrinsic error on the computed transition energies of guanine monomer. FrDEX spectra are fairly close to the reference TD-DFT ones, allowing a significant advance with respect to a more standard excitonic Hamiltonian. We also show that the ECD spectra are sensitive to the inclusion of the inner K⁺ cation in the calculation.

KEYWORDS

ECD, excitonic model, fragment diabatization, guanine quadruplexes

1 | INTRODUCTION

Nucleic acids (NAs) are chiral species, both due to the intrinsic chirality of the sugars and the helical

arrangement of the nucleobases, making electronic circular dichroism (ECD)¹ a widely used technique to characterize their structural behavior.^{2–8} Among the different NA secondary structures, ECD is particularly informative

[This article is part of the Special issue: Chiral Materials. See the first articles for this special issue previously published in Volumes 34:12, 35:2, 35:3 and 35:4. More special articles will be found in this issue as well as in those to come.]

This is an open access article under the terms of the [Creative Commons Attribution-NonCommercial](https://creativecommons.org/licenses/by-nc/4.0/) License, which permits use, distribution and reproduction in any medium, provided the original work is properly cited and is not used for commercial purposes.

© 2023 The Authors. *Chirality* published by Wiley Periodicals LLC.

for monitoring the static and dynamical behaviors of guanine quadruple helices (hereafter GQs). This peculiar structure can be adopted by Guanine-rich DNA and RNA sequences and has been the focus of intense research activity in recent years. Indeed, GQs have been shown to be present in living cells^{9–11} and have been identified as important therapeutic targets,^{12,13} since they are likely involved in many key biological processes.¹⁴

As schematically depicted in Figure 1 below, the repeating units of GQs are four guanines (Gs) arranged in a plane (tetrad) connected by Hoogsteen-like hydrogen bonds and stabilized by the coordination of inner cations, for example, K^+ and Na^+ .^{11,15,16} The bases of the tetrads can belong either to different NA strands (e.g., bimolecular, tetramolecular GQs) or to a single NA strand. In this latter case, tetrads are connected by loops made up of additional nucleobases. Gs can be in syn- or anti-conformation with respect to the glycosidic bond and, considering the relative strand orientations, can have parallel (all the strands have the same orientation), antiparallel (two parallel and two antiparallel G strands), and (3+1) hybrid (three parallel and one antiparallel G tracts) GQ topologies. Taking into account that loops can also adopt different conformations, GQs exhibit a large structural diversity despite their thermal stability, and many factors (sequence, the nature of the coordinated ions, and temperature) determine the final folding topology.^{15,16} The asymmetric arrangement of the bases in each step affects the ECD signal so that each topology has a distinct ECD signature. These characteristics have

made ECD the elective technique to identify the presence of GQs and to characterize their folding topology, their thermal stability, and their folding/unfolding dynamics. For a detailed review of the experimental papers in the field, see earlier studies,^{7,8} and references therein. More recently, useful procedures have also been proposed to obtain quantitative secondary structural and topological information for GQs from their ECD spectra, for example, the number of anti-anti, syn-anti, or anti-syn base steps.²

Concurrently, very interesting nonempirical interpretative models of the experimental ECD signal have been proposed.^{6,17,18} A widely used one is based on the definition of the polarity of each tetrad. In their own words, Spada, Randazzo, and colleagues state that “A simple exciton coupling approach or more refined quantum mechanical (QM) calculations allow to interpret the different CD features in terms of different stacking orientation (head-to-tail, head-to-head, tail-to-tail) between adjacent G-quartets”.¹⁸

When compared with the huge amount of experimental results available, the number of computational studies focussing on the electronic spectra of GQ, or, more generally, on their photoactivated behavior is quite limited.^{19–22} Actually, the size of GQ (at least 8–12 Gs, without considering phospho(deoxy)ribose backbone, counter-ions, and loops) is extremely challenging for QM calculations. Moreover, the simulation of the electronic spectra (absorption or ECD) up to the UVB-UVC region (~ 220 nm) requires the calculation of several dozens of

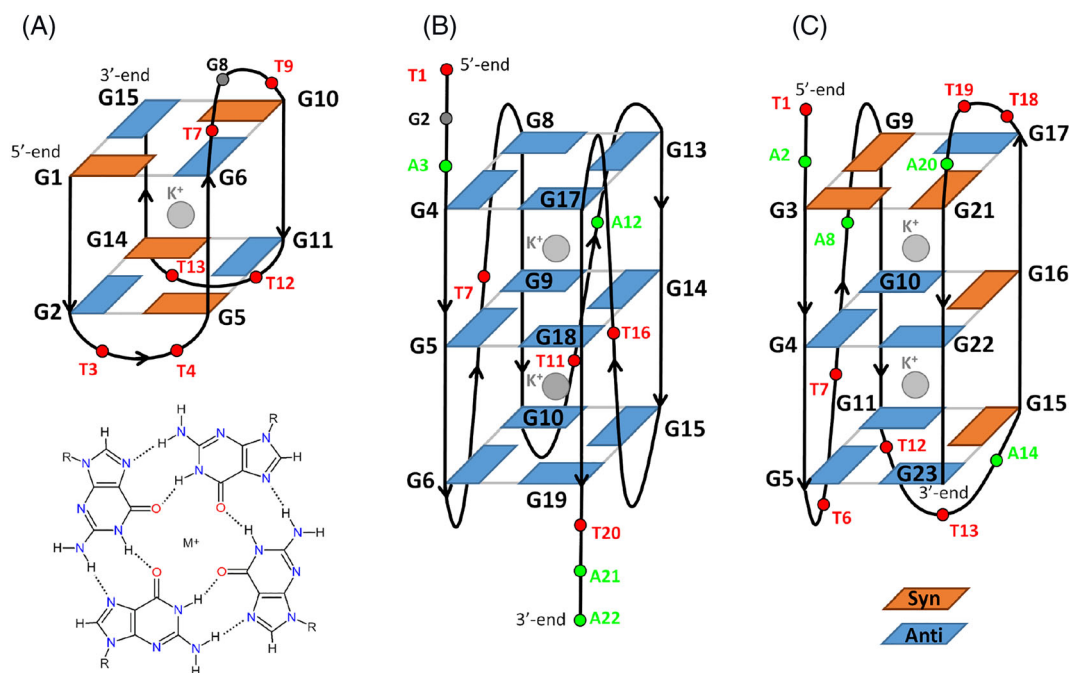


FIGURE 1 Schematic drawing of the guanine quadruples (GQs) investigated in this study: (A) thrombin binding aptamer (TBA). (B) c-Myc promoter (c-Myc). (C) Human telomeric sequence (Tel23). The schematic drawing of a “tetrad” is shown below TBA.

excited states, further increasing the computational cost. It is not surprising, therefore, that many studies of the ECD spectra of GQs have resorted to excitonic models,^{6,23–25} which describe the excited states of GQs on the basis of local excitations (LEs) of guanine and their couplings. From this perspective, GQs are a suitable playground for the assessment and the refinement of excitonic Hamiltonians, since the close stacking between the Gs could defy many of their more commonly adopted approximations, for example, the lack of coupling with excited states with charge transfer (CT) character or the dipolar approximation.

In this context, we have recently proposed a protocol that employs a fragment-based diabaticization (FrD), to parameterize a generalized excitonic (Ex) Hamiltonian, FrDEx, which describes the interplay between LE and CT states and is aimed at the study of closely stacked multi-chromophore assemblies (MCAs). In its first application, FrDEx has been adopted to simulate the absorption and ECD spectra of two GQs: a human telomeric sequence in antiparallel basket-type topology; and the tetramolecular parallel GQ formed by the TGGGGT sequence,²⁶ providing spectra similar to those of the reference QM method (time-dependent density functional theory [TD-DFT] using the M052X functional), and in fairly good agreement with the experimental one. Moreover, when coupled with Molecular Dynamics (MD) simulations, FrDEx has provided useful information on the effect that the loops and thermal fluctuations of the structure have on the ECD spectral signal.²⁷ Very recently, we have also profitably used FrDEx to compute the ECD spectra of a GC B-DNA duplex.²⁸ These promising results have however been obtained only on two particular systems, a sample too small to fully assess the performances of FrDEx in simulating the electronic spectra of GQs and test its limitations.

In this study, we thus apply FrDEx to study three additional different sequences, which are known to adopt in solution the three commonly found topologies, namely, antiparallel, parallel, and hybrid (or 3+1), each one characterized by a typical ECD signature. In detail, as shown in Figure 1, we have computed the ECD spectra of the thrombin binding aptamer (GG-TT-GG-TGT-GG-TT-GG sequence, hereafter TBA) of a sequence of the human c-Myc promoter (TGA-GGGT-GGGT-A-GGGT-GGGT-AA, hereafter c-Myc) and of a 23-nucleotide fragment of the human telomeric sequence (TA-GGGTTA-GGGTTA-GGG, hereafter Tel23), based on their experimental structures. In the presence of K⁺ ions, TBA adopts an antiparallel chair-type topology,^{29,30} c-Myc a parallel,³¹ and Tel23 a hybrid-1 one.³²

Besides giving useful information on the most suitable protocol to be followed when applying FrDEx (and

more generally any excitonic model) to GQs, this study is aimed to provide additional insights into the different chemical–physical effects determining the spectral line-shape. In particular, we shall focus on the role played by the inner coordinated cation and on the possible contribution of the guanine bases present in the loops. Finally, although a thorough assessment of the performances of TD-DFT is well beyond the scope of the present paper, we can gain useful information on the potentialities, and the limitations, of this method, in the study of optical properties of GQ.

2 | METHODS

2.1 | FrDEx procedure

In the FrDEx model, we write an excitonic state k in terms of LEs on N_{mol} individual monomers and CT states between dimers:

$$|\Psi^k\rangle = \sum_m^{N_{\text{mol}}} \sum_\alpha^{N_{\text{loc}}} C_m^{\alpha,k} |L_\alpha^m\rangle + \sum_m^{N_{\text{mol}}} \sum_{n \neq m}^{N_{\text{mol}}} \sum_\gamma^{N_{\text{CT}}} C_{mn}^{\gamma,k} |CT_\gamma^{m \rightarrow n}\rangle \quad (1)$$

where for each monomer m , the index α labels the N_{loc} possible LEs (L_α^m) with corresponding coefficient $C_m^{\alpha,k}$. The index γ identifies the N_{CT} different types of CT states ($CT_\gamma^{m \rightarrow n}$) where an electron is transferred from monomer m to monomer n , with corresponding coefficient $C_{mn}^{\gamma,k}$.

In the basis of these LE and CT states, we split the Hamiltonian into an intramolecular part H_{intra} and intermolecular part H_{inter}

$$H_{\text{FrDEx}} = H_{\text{intra}} + H_{\text{inter}}. \quad (2)$$

In the intramolecular part, we have the LE energies and the couplings of different LEs on the same monomer. These couplings are zero for adiabatic LE states of an isolated monomer but become nonzero in a MCA due to the electrostatic and polarization effects of the surrounding monomers and/or the overlap with their molecular orbitals, causing LEs defined on an isolated monomer to mix when other monomers are present nearby. Furthermore, whereas in “standard” excitonic models the LE energies are typically set to be equal to those of the isolated monomer, our Hamiltonian accounts for the possible effect of the surrounding monomers in a MCA. Previously, we have referred to both these phenomena as a “perturbation” of the monomeric LEs.^{26,27} In the intermolecular part, we have all the terms involving more

than one monomer, that is, the CT energies, LE-CT and CT-CT couplings, as well as the LE-LE couplings for LEs located on different monomers (usually referred to as excitonic couplings). The full expressions for H_{intra} and H_{inter} have previously been written^{26,27} and are also included in the supporting information (SI) Section S1.

These energies and couplings are calculated via a fragment diabatization (FrD) technique, where we define diabatic states of some supramolecular complex (SC) consisting of N_{frag} fragments, a subset of the total N_{mol} monomers, using as reference states either the adiabatic states of the fragments (for LEs) or orbital transitions between the fragments (for CT states).

As derived and illustrated previously,^{26,33} the diabatic states $|\mathbf{d}\rangle$ are then obtained by

$$\begin{aligned} |\mathbf{d}\rangle &= |\mathbf{a}^{\text{SC}}\rangle \mathbf{D} \\ &= |\mathbf{a}^{\text{SC}}\rangle \mathbf{S}^T (\mathbf{S}\mathbf{S}^T)^{-\frac{1}{2}} \end{aligned} \quad (3)$$

where $\mathbf{S} = \langle \mathbf{R}^{\text{frags}} | \mathbf{a}^{\text{SC}} \rangle$ is the overlap of the reference states of the fragments ($|\mathbf{R}^{\text{frags}}\rangle$) with the adiabatic states of the SC ($|\mathbf{a}^{\text{SC}}\rangle$). The diabatic energies and couplings can then be calculated from the transformation matrix \mathbf{D} applied to the diagonal matrix of adiabatic energies of the SC $H(\mathbf{a}^{\text{SC}})$. The diabatic dipole moments may similarly be obtained by application of \mathbf{D} to the diagonal matrix of adiabatic dipole moments. The flexibility of the FrDEX method lies in the ability to choose a SC of any size with an arbitrary number of fragments to compute the couplings and energies, so as to balance computational cost and accuracy, avoiding, at the same time, any double-counting effect. Indeed, different sizes of SC may be chosen to parameterize H_{intra} and H_{inter} , and as previously with GQs, we choose dimers for H_{inter} ²⁶ and use either a single “Strand” or a “Tetrad” of guanine bases for H_{intra} .

These choices are illustrated in Figure 2, using c-Myc as an example GQ.

The FrDEX spectra will be compared also with those obtained by a more “standard” excitonic approach, that is, a Frenkel Hamiltonian with Coulombic couplings (FHC), constructed by computing the excitonic couplings based on the Coulomb interaction of the full transition densities of G bases and taking LE energies as those for an isolated monomer.^{24,25}

2.2 | Computational details

2.2.1 | Reference QM calculations

As anticipated above, the simulation of the ECD spectrum of a GQ requires the calculation of a large number of excited states for a system containing at least ~ 150 atoms. The only viable option, in order to combine computational feasibility with fairly good accuracy, is TD-DFT. The limitations of TD-DFT are well-known, for example, in the treatment of the electronic transitions with CT character,^{34,35} although they can be partially overcome by choosing a suitable functional.³⁵ We here resorted to M052X,³⁶ a functional we have already profitably used in studying the photophysics and photochemistry of DNA,^{37,38} along with the 6-31G(d) basis set. It should be noticed that, since M052X does not reach 100% exact exchange limit at large distances, it could fail in correctly describing the CT transitions between very distant chromophores. However, here we only consider the closest nearest-neighbor pairs, because as reported previously these give the largest contribution.²⁶

In order to include the effect of water solvent, we adopted a computationally convenient implicit solvation scheme, the polarizable continuum model (PCM).³⁹ The

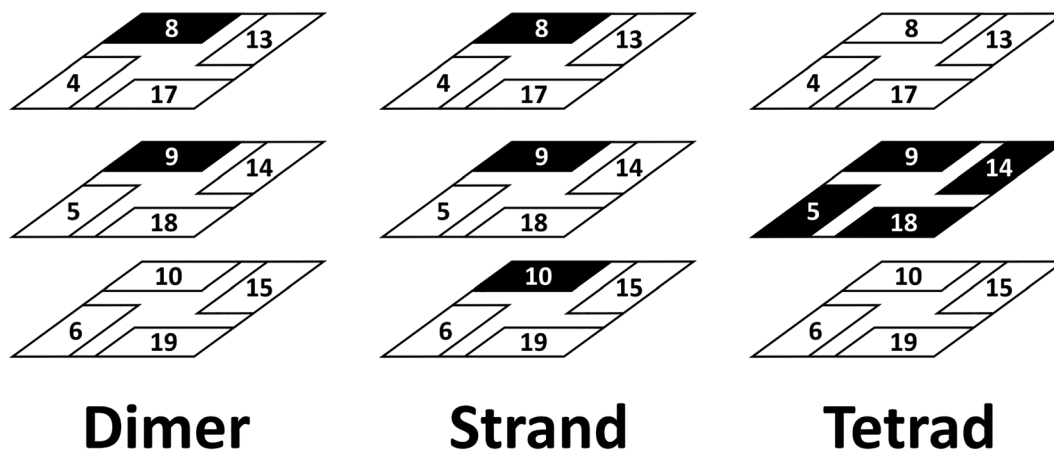


FIGURE 2 Illustration of different supramolecular complexes chosen for diabatization to parameterize the FrDEX Hamiltonian (colored rectangles). Guanines for which FrDEX parameters are obtained from the specified subset of guanine quadruple (GQ) are highlighted in black. The c-Myc sequence, see Figure 1, has been taken as example.

TD-DFT/PCM calculations were performed in Gaussian 16.⁴⁰ We checked by visual inspection (one case is reported in Figure S13 in the SI) that with the standard settings of the code, the PCM cavity is built in a way that no dielectric is placed between the stacked bases. We further checked that the TD-DFT results are similar with larger cavities, obtained by increasing the scaling factor α from 1.1 (default) to 1.2 and even in the gas phase (Figure S14). In the computation of the reference diabatic LE and CT states $|\mathbf{R}^{\text{frags}}\rangle$ and the states they are projected onto $|\mathbf{a}^{\text{SC}}\rangle$, we include the other bases and the inner stabilizing cation (K^+) at the molecular mechanics (MM) electrostatic level, via restrained electrostatic potential (RESP) charges, computed at the same level of theory. The RESP charges were included outside of the PCM cavity, and a check was made to ensure that placing them inside the cavity did not significantly affect the parameters obtained (see Table S4). Test calculations on TBA (see Figure S12 in the SI) also show that the computed spectra do not significantly change when the RESP charges of the G bases are not considered in the calculation. The diabatization was performed by our freely available code, Overdia.⁴¹ For the FHC approach, the Coulombic couplings between LEs were evaluated using the “EET” option in Gaussian⁴² which utilizes transition densities and solvent effects with PCM. The PCM cavities were constructed using the “FragmentCavity” option, which builds a PCM cavity for each pair of fragments when evaluating the excitonic coupling. This allows maximum correspondence to the FrDEx approach, which utilizes PCM cavities in a similar manner and also is a suitable option for large multichromophoric systems like those studied in this paper.²⁴

For all the FrDEx and QM calculations, we have considered only the G bases. All the atoms in sugar-phosphate backbone are stripped off except for C1' of deoxyribose sugar, which is substituted by a methyl group. The 9-methyl-guanine, optimized at the M052X/6-31G(d)/PCM(water) level of theory, then replaces the guanine geometries from the PDB structures, by minimizing the RMSD between them. In our previous studies, we have analyzed the possible effect of this approximation on the computed spectra.²⁷

For FHC calculations, 10 excited states are calculated for each fragment, and then we used the first two bright transitions of each fragment in building the Hamiltonian, with the LE energies those of monomeric guanine without any surrounding RESP charges. In case of FrDEx, the excited states calculated for monomer, pair, strand, and Tetrad are 10, 40, 30, and 40, respectively. These calculations are used in the FrD where the H_{intra} and H_{inter} terms are computed, which include two LE states for each G and four CT states for each nearest-neighbour

TABLE 1 Comparison of the effects considered in the FHC and FrDEx models used in this work.

Effect	FHC	FrDEx
Full Coulombic LE-LE excitonic couplings	✓	✓
PCM water	✓	✓
CT states	✗	✓
MM surrounding bases	✗	✓
Monomeric LE perturbation	✗	✓

Abbreviations: CT, charge transfer; FHC, Frenkel Hamiltonian with Coulombic couplings; LE, local excitation; MM, molecular mechanics; PCM, polarizable continuum model.

pair. A comparison of the effects incorporated in the FHC and FrDEx models in this work is shown in Table 1. We note that some of the effects accounted for by FrDEx are also considered in other ab initio excitonic models in the literature.^{43–46}

In the next subsection, we discuss some computational strategies we adopted to take into account the possible source of inaccuracy in our reference QM calculations.

2.2.2 | Simulation of the spectra

The spectra were computed using a modified version of the EXAT code,²⁴ and we utilize the rotatory strength in velocity gauge to compute ECD spectra, to avoid any origin dependence.^{26,27} The simulation of the ECD spectrum in UVB-UVC region requires the calculation of ≥ 40 excited states, making unfeasible a proper inclusion of vibrational and thermal effects in the lineshapes. They are phenomenologically accounted by simply convoluting the “stick” contribution of each excited state by a Gaussian, with half-width-half-maximum (HWHM)=0.18 eV. However, as shown by the test calculations reported in the SI, our conclusions do not depend on the value assigned to this latter parameter.

The expected accuracy of the computational method for GQs is clearly linked to the one observed for the monomer species G. In this respect, we should notice that the two lowest energy bright excited states (L_a and L_b) of 9methyl-guanine are blue-shifted by 0.75–0.85 eV with respect to the maxima of the experimental absorption band of guanosine in water at the PCM/TD-M052X/6-31G(d) level of theory, as shown in Figure S5 and in Table S1 of the SI. A part of this shift (0.1–0.2 eV) is due to the absence of thermal and vibrational effects in our treatment, which lead to a systematic red-shift of the band maxima with respect to the vertical transition energies.^{47,48} A significant part of the error is, however, due to the limitations of our computational approach (e.g., density functional and basis set). This is not a very

problematic issue for this study, whose main purpose is to assess the reliability of FrDEx with respect to the reference QM calculation. On the other hand, it is clearly interesting to verify if the computed spectra are consistent with the experimental ones. Therefore, in order to allow an easier comparison with the experiments, we shall report computed spectra red-shifted by 0.8 eV, that is, the error made in simulating the absorption spectrum of the monomer with the same level of theory.

As a matter of fact, the test calculations described below will suggest that the main source of error in the calculation of the ECD is the description of the monomer and not the treatment of the electronic interactions in the GQ.

Finally, it is noteworthy that PCM/M052X/6-31G(d) calculations quite significantly overestimate the intensity of the L_b transition with respect to that of L_a (see Figure S5 in the SI) and, in the following, we will explore the performance of a very simple strategy to correct for this error.

3 | RESULTS

3.1 | TBA, antiparallel topology

The ECD spectrum of TBA (Figure 3) is typical of antiparallel GQs, featuring a strong positive peak at ~ 290 nm, a negative one at ~ 270 nm and a positive one

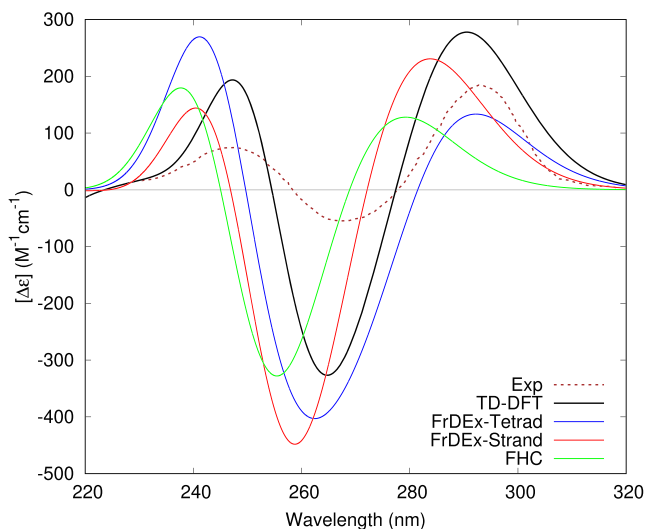


FIGURE 3 Computed electronic circular dichroism (ECD) spectra of thrombin binding aptamer (TBA) guanine quadruple (GQ) using time-dependent density functional theory (TD-DFT), Frenkel Hamiltonian with Coulombic coupling (FHC), and FrDEx (by using both “strand” and “tetrad” approaches). Intensity is in molar extinction ($\Delta\epsilon$). Experimental spectra reported in Gray et al.,³ are multiplied by a factor of 15 to be in GQ rather than nucleotide concentration (see text for details).

at ~ 250 nm. The latter two peaks have similar intensity, whereas the one in the red is \sim three times stronger. The shape of the spectrum computed by TD-M052X/6-31G(d) is similar to the experimental one, and once shifted by -0.8 eV, the position of their peaks is very close.

In order to allow a more direct comparison with our calculations, the intensity of the experimental spectrum, expressed in molar extinction per nucleotide,³ has been multiplied by 15 to express it instead relative to GQ concentration. Overall, the computed intensity for the peak at ~ 290 nm is in good agreement with the experimental one, especially when considering that thermal fluctuations, whose inclusion is outside the scope of this paper, would also affect the intensity of the spectrum.²⁷

Concerning the relative intensity of the peaks, the most significant discrepancy between the TD-M052X and the experimental ECD spectra is the significant overestimation of the intensity of the negative feature at ~ 270 nm. Since this feature is associated with L_b excited states, it is possible that this error can be traced back to the overestimation of the relative intensity of L_b transitions in the G monomer. This is confirmed by the test calculations reported below. The FrDEx spectra are in good agreement with the reference QM one. The position of the peaks of the “tetrad spectrum” nicely agrees with the QM reference. The only significant discrepancy concerns the intensity of the red-wing positive lobe. The “strand” approach provides instead less accurate results, with larger errors in the position of the peaks. In TBA, there are indeed only two tetrads, so it seems that the possibility of including the effect of the stacking on H_{intra} (as in the “strand” approach) is less important than treating the effect of the hydrogen bonding in the tetrad at a QM level (as in the “tetrad” procedure).

In the SI, I we also show that the inclusion of the G bases present in the loop (G8 in Figure 1A) does not significantly affect the computed ECD spectrum, but for a small increase of the relative intensity of the negative peak at ~ 260 nm. Actually, in the experimental structure considered, the stacking between G8 and the other G bases is quite poor (see Figure S1 in the SI). On the other hand, the relative position of the extra G8 base with respect to the G-tetrad is quite different in the various structures of the free TBA experimentally determined.^{29,30,49} Finally, in Figure S14 of the SM, we also show that the ECD spectrum varies only moderately if we increase the size of the PCM cavity using a value of 1.2, larger than default 1.1 for the scaling factor α . We also show in Table S4 that the parameters of the FrDEx Hamiltonian change only slightly if, in the fragment computations, we do not include the RESP charges within the PCM cavity (the standard approach we adopt)

or if we include the RESP charges inside the PCM cavity (Table S4).

Figure 3 shows that FrDEx spectra are much closer to the reference QM results than that obtained by a standard excitonic Hamiltonian (FHC; see Section 2.1) which is quite significantly blue-shifted with respect to the QM reference. Furthermore, as analyzed in the SI, the standard excitonic Hamiltonian cannot reproduce the large hypochromic effect in the absorption spectra, which is associated with the formation of the GQ.

According to our calculations, the inclusion of the inner K^+ ion has a remarkable effect on the computed spectra. As reported in Figure 4, the presence of K^+ red-shifts the positive lobe in both the FrDEx and in the QM spectra by 10–15 nm, improving the agreement with the experimental one.

Finally, looking for simple recipes to improve the accuracy of the parameters of our FrDEx Hamiltonian, we explored the possibility of correcting the errors intrinsic to the TD-DFT reference of the monomer. In this direction, in Figure 5, we present the result of two exploratory calculations where we modified the energy of the LEs and the intensity of L_b transition, so to better fit their experimental counterpart in the G monomer. As shown in Figure 5, the spectrum computed for TBA, by simply shifting the energy of the LEs by -0.80 eV (and without any additional changes) is very similar to the one computed with the original FrDEx parameters and then

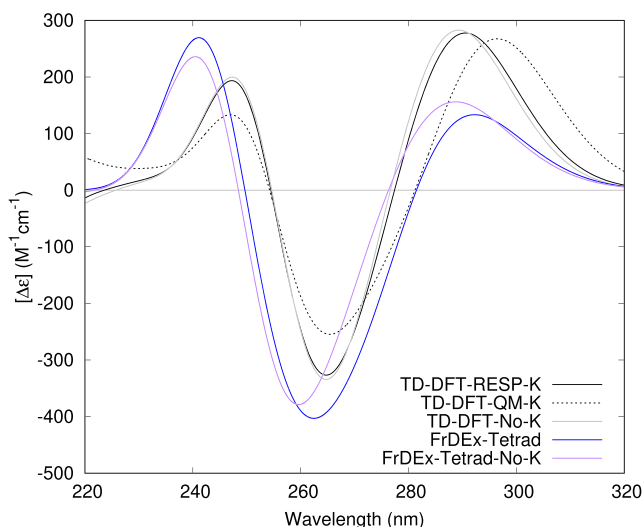


FIGURE 4 Electronic circular dichroism (ECD) spectra of thrombin binding aptamer (TBA) computed, at time-dependent density functional theory (TD-DFT) or at FrDEx level, including or not the K^+ central ion in the calculation. Intensity is in molar extinction ($\Delta\epsilon$). Black dotted line: K^+ treated at the quantum mechanical (QM) level; black (TD-DFT) and blue (FrDEx-“tetrad”) lines: K^+ treated at the classical level; gray and mauve lines (no- K): K^+ is not included.

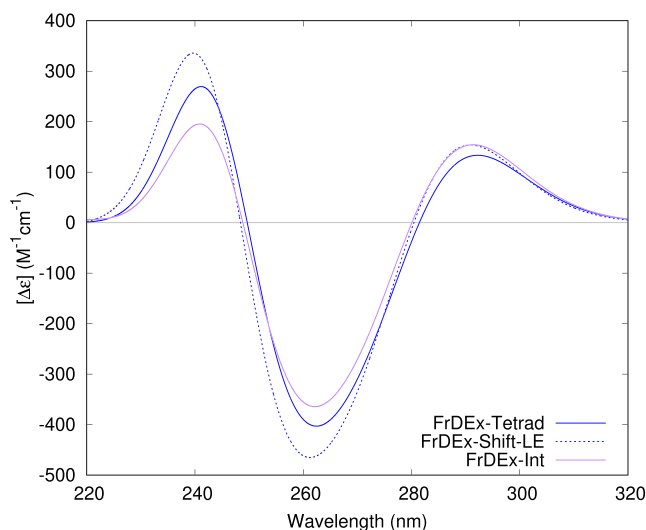


FIGURE 5 Electronic circular dichroism (ECD) spectra of thrombin binding aptamer (TBA) computed by FrDEx and shifted afterward by -0.80 eV (blue) are compared with ones computed after simply shifting the local excitation (LE) states of G by -0.80 eV (dotted-blue) or decreasing the module of the transition electric dipole moment of L_b states by 30% and then shifting the spectrum by -0.80 eV (purple). Intensity is in molar extinction ($\Delta\epsilon$).

shifted by the same amount. On one side, this finding indicates that the main error in the position of the spectrum is due to the error in the LEs energies, and on the other hand, it suggests that the role of CT states is quite minor, since clearly the extent to which they can mix with LEs is strongly affected by the large shift we applied.

In a second test in Figure 5, we decreased the module of the electric transition dipole moment of L_b by 30% so to better match the relative intensity of L_a and L_b transition in guanosine.⁵⁰ The result is a decrease in the intensity of the negative peak at ~ 260 nm which improves the agreement with the experimental spectra.

3.2 | Human c-Myc promoter, parallel topology

c-Myc promoter, a transcription factor involved in many key cellular processes,⁵¹ exhibits the typical ECD spectrum of parallel GQs (see Figure 6). We observe an intense positive peak at ~ 260 nm, and a negative one, of comparable intensity, at ~ 240 nm. Once shifted, the TD-DFT spectrum is in good agreement with the experimental one, for what concerns both the position and the relative intensity of the two main peaks. The lineshape of the FrDEx “strand” spectrum is also consistent with the experimental one, though the width of the positive band at 240 nm is larger than the experimental and the QM

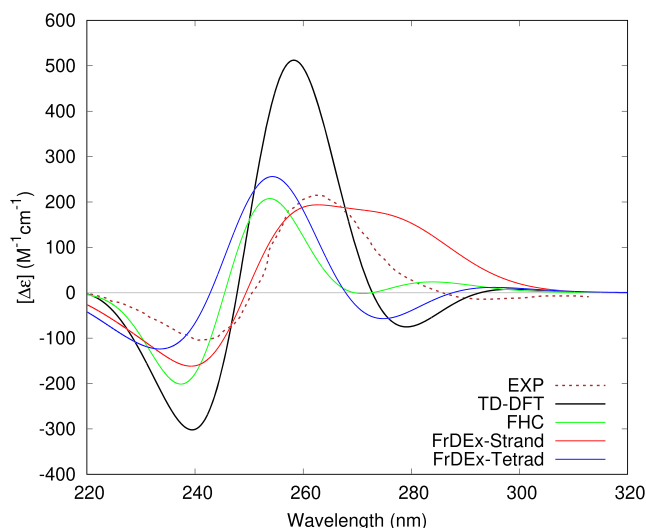


FIGURE 6 Computed electronic circular dichroism (ECD) spectra of c-Myc guanine quadruple helix (GQ) using time-dependent density functional theory (TD-DFT), Frenkel Hamiltonian with Coulombic couplings (FHC), and FrDEx (with “strand” and “tetrad” approaches). The reference experimental spectrum from del Villar-Guerra et al² is also shown. Molar extinction $\Delta\epsilon$ given relative to GQ concentration.

ones. The shape of the “tetrad” spectrum is in better agreement with the QM reference but for a weak blue-shift and the overestimation of the intensity of the small negative peak appearing in the low-energy part of the spectrum. It should be noted that such a peak would be largely washed out by choosing a slightly larger broadening (see Figure S9 in the SI). The “strand” spectrum, though correctly reproducing the position and the relative intensity of the two QM peaks, overestimates the width of the positive band on the red-side. For c-Myc, there are bases on other strands that are also quite closely stacked, and as the “strand” approach only accounts for the LE perturbation among stacked bases in the same strand, it could be missing this effect. These trends are similar to that found for the tetramolecular parallel GQ formed by TGGGGT sequences,²⁶ suggesting that they could be due to “intrinsic” limitations in the description of this topology at FrDEx level. In any case, also for c-Myc, FrDEx spectra are much closer to the reference TD-DFT one than those provided by a standard excitonic Hamiltonian.

As shown in the SI, the inclusion of K^+ in the FrDEx calculations impacts the intensity of the different bands but has a limited effect on their position, a similar effect is seen when the K^+ ion is described at the QM level in the TD-DFT spectrum (see Figure S8 in the SI). However, as shown in the SI (Figure S4), including the contribution of G2 (the G base in the loop; see

Figure 1B) has a more significant effect on the spectrum, leading to a further broadening of the positive low-energy band.

3.3 | Human telomeric sequence with hybrid-1 topology

In the presence of K^+ ions, human telomeric sequences are known to adopt a hybrid (3+1) topology. Figure 7 shows that the ECD spectrum of the sequence Tel23 is quite peculiar, with a broad positive band above 260 nm and a weak negative lobe at ~ 240 nm. Two shallow maxima can be recognized in the positive band, at ~ 270 and ~ 290 nm. After applying a 0.80 eV red-shift, as previous, the PCM/TD-M052X spectrum closely resembles the experimental one, with two maxima clearly present in the positive band, followed by a less intense negative feature at high energy. In this respect, it is important to remind that the shape of the computed spectrum in the high-energy tail could be affected by the existence of higher-lying excited states not included in our calculation.

The performance of FrDEx model, for this structure, is worse than that found for TBA and c-Myc. Indeed, both according to “tetrad” and “strand” approaches, the positive/negative alternation in the reference QM spectrum is reproduced, but the positive band is much less

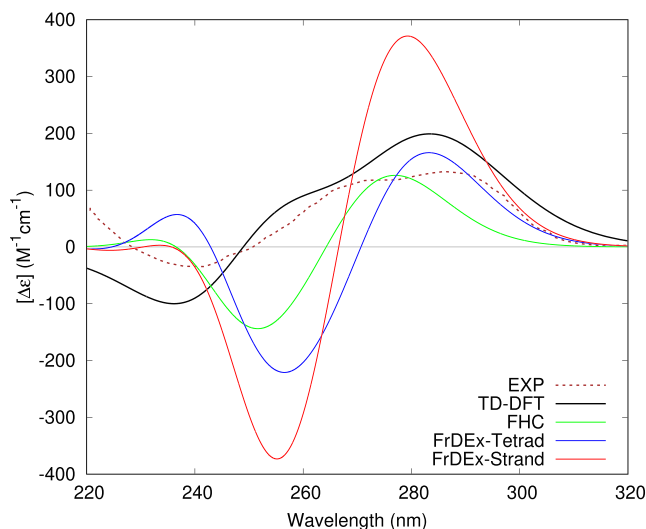


FIGURE 7 Computed electronic circular dichroism (ECD) spectra of Tel23 guanine quadruple (GQ) using time-dependent density functional theory (TD-DFT), Frenkel Hamiltonian with Coulombic couplings (FHC), and FrDEx. The reference experimental spectrum from del Villar-Guerra et al² is also shown. Molar extinction $\Delta\epsilon$ given relative to GQ concentration.

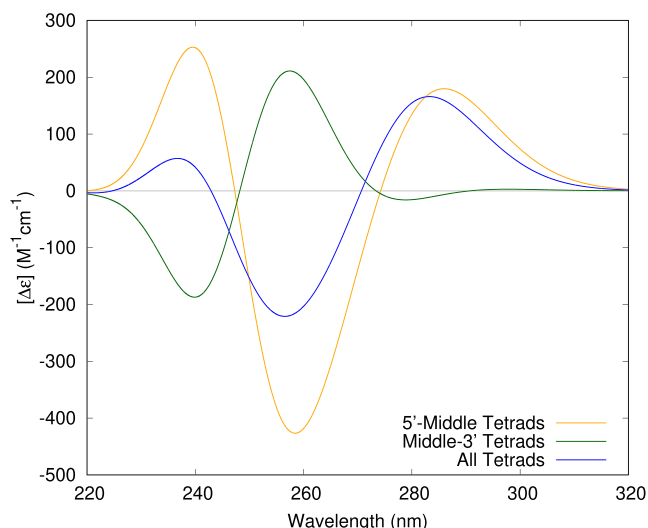


FIGURE 8 Computed electronic circular dichroism (ECD) spectra for the different pair of stacked tetrads in Tel23 guanine quadruple (GQ), using FrDEX.

broad than the QM reference and, correspondingly, the negative one is too intense and red-shifted.

Looking for an explanation of the worse performance of FrDEX, in Figure 8, we report separately the contribution to the ECD signal of the interaction between the tetrad at the 5' end (see Figure 1) and the central one, (5'-middle tetrads curve in Figure 8) and between the central tetrad and that at the 3' end (middle-3' tetrads curve in Figure 8).

These results indicate that the two positive peaks observed both in the experiment and in the reference TD-DFT calculation can be associated with the 5'-middle and middle-3' tetrads. This result is in line with the “traditional” interpretation of the GQ spectra in terms of stacking between tetrads of different polarity.³ Actually, the decomposition of the CD spectrum of 3+1 hybrid structure in the contribution of the spectra from pair of tetrads in head-to-tail and head-to-head arrangements has been already proposed in the literature.⁶

However, FrDEX overestimates the energy separation between the two positive peaks of the 5'-middle and middle-3' tetrads, so that the positive peak of the middle-3' tetrad is overwhelmed by the negative one of the 5'-middle tetrad, since both fall at ~ 260 nm. It is also possible that the intensity of the negative contribution of the 5'-middle tetrad is overestimated.

In the SI, we show the “stick” ECD spectra computed at the TD-M052X and at the FrDEX “tetrad” level. It can be noticed that FrDEX misses two transitions with quite large positive rotatory strength, which would contribute to the maximum at ~ 260 nm. They are associated with

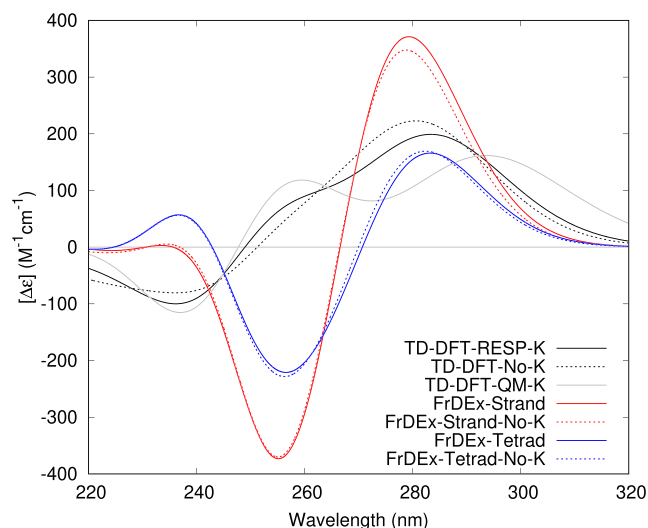


FIGURE 9 Computed electronic circular dichroism (ECD) spectra of Tel23 guanine quadruple (GQ) in the presence restrained electrostatic potential (RESP) charges of K compared with ECD spectra calculated without K using time-dependent density functional theory (TD-DFT) and FrDEX.

pairs of bases on different strands, whose interaction is treated with H_{inter} , but not considered when computing H_{intra} in FrDEX. It could be possible, therefore, that this interaction modifies the intrinsic properties of the LEs on the involved bases (i.e. energies, intramonomer LE-LE coupling, dipoles) in a manner not captured by either the “strand” or “tetrad” approaches. In any case, also for Tel23, the FrDEX spectra are more accurate than those obtained at the FHC level or by using other approximate methods.³

We further analyzed for Tel23 the effect of the inclusion of K^+ ions. Figure 9 shows that it slightly improves the agreement with experiment, at least in the TD-DFT spectrum. If the K^+ is not considered in this calculation, the intensity of the positive peak at ~ 260 nm decreases, and only one band peaking at ~ 280 appears. However, when the K^+ ion is described at the QM level, the spectrum significantly changes. As shown in Figure 9, the separation of the two positive peaks increases, mainly due to a ~ 10 nm red-shift of the lowest energy one.

4 | CONCLUDING REMARKS

In the study, we have further assessed the performance of the protocol we have recently developed to compute electronic spectra of closely stacked MCA, by simulating the ECD spectra of three GQs of different topologies. Our approach, FrDEX, exploits a FrD of reference QM calculations to parameterize a generalized excitonic

Hamiltonian that describes the interplay between LEs and CT states.

For the three GQs examined, FrDEx ECD spectra are in fairly good agreement with the reference QM ones. The shapes are similar, and in many cases, the predicted peaks are within ~ 10 nm.

The most relevant discrepancies with respect to the TD-M052X spectral shape concern the relative intensity of the low-energy positive band in antiparallel TBA and, especially, the presence of a single positive band in (3+1) Tel23, that is, lacking the two shallow maxima at ~ 260 and ~ 290 nm. These errors are likely due to the contribution coming from the interactions of bases on different strands. In both our “strand” and “tetrad” strategies in FrDEx, we consider these interactions in the H_{inter} but not in H_{intra} , that is, we do not consider how these interactions can affect the intrinsic properties of the LEs on the involved bases.

In all examined cases, FrDEx provides spectra much closer to the reference QM ones than those obtained by a standard excitonic model, which computes the couplings using only the Coulombic interaction (plus PCM effects). It is worth highlighting that the latter does also not reproduce the hypochromism of the absorption spectra, which is, on the contrary, nicely captured by FrDEx (see SI). This study thus confirms that, in closely stacked MCA, the FrDEx approach is particularly effective. It is indeed important to consider the effect of the surrounding monomers on the LEs of the monomer, to describe couplings beyond a simple Coulombic approximation (even if considering the full transition densities), accounting for the possible overlap of the electronic densities and to include the coupling with CT states. This latter effect has been investigated in our previous contributions, analyzing in detail the spectra obtained for several shorter fragments of GQs of different topologies.^{26,27} We have shown that the inclusion of CT states is crucial to reproduce the reference QM spectra in the high-energy region, that is, below 250 nm, where their mixing with bright states is larger. Moreover, for closely stacked bases, CT states also provide a nonnegligible contribution to the lowest energy part of the spectrum. In the SM, we report the values of the FrDEx parameters computed for TBA, and also in this case, the CT states involving quite closely stacked bases fall 0.2–0.3 eV on the blue with respect to L_b LE (see Figure S15), with a nonneglectable coupling with both LEs (Figure S17).

Our study highlights the effect of K^+ inner cations on the spectral shapes, which is more evident on the redwing of the spectrum, confirming the influence of the closely coordinated cations on L_a transitions.²² Interestingly, especially in two of the examined GQs, the effect

on the spectra cannot be reduced to the electrostatic interactions, and thus, it cannot be accurately modeled at a classical level. An explanation for this finding could be due to the significant CT between the K^+ ion and the surrounding bases. In fact, the positive charge of the K atom, according to a simple Mulliken population analysis, is ~ 0.5 . This effect, which cannot be captured at a classical level, can significantly affect the coupling between the excited states of Gs (both LE and CT states). The influence of the K^+ ion on the spectra will depend on its fluctuations within the GQ. In this respect, especially when studying ions more mobile than the bulky K^+ (such as Na^+)^{52,53} proper inclusion of conformational averaging effects could be important.

Our calculations confirm that the bases in the loop can affect the ECD lineshapes, in agreement with the indications of our previous study on antiparallel Tel21.²⁷ On the other hand, as loops can be much more flexible than the “tetrad core”,^{54–57} considering only one structure as we did in this study, could in principle dramatically decrease the reliability of the computational indications, and integration with MD simulations is recommended.

This study provided us also an interesting opportunity to test the reliability of TD-DFT calculations in predicting the ECD spectra of large closely stacked MCAs such as GQs. Keeping in mind that the use of a functional allowing proper treatment of CT transitions is mandatory, the TD-M052X spectra reported here exhibit spectral shapes in nice agreement with experiments. The most important discrepancy with respect to the experiments concerns a large, almost uniform, blue-shift of the TD-M052X spectra. The magnitude of this shift, ~ 0.80 eV, is, however, very similar to that needed to reproduce the absorption spectra of the monomeric species, that is, guanosine in water, at the PCM/TD-M052X/6-31G(d) level. In fact, simply shifting the values of the LE energies by ~ 0.80 eV in the FrDEx Hamiltonian leads to obtaining spectra close to the experimental ones, without any additional shift. This result confirms that the main error of TD-DFT/M052X is associated with the description of the monomer and not with the treatment of the interactions between excited states in the GQ. Similar considerations apply to another possible source of error, sometimes overlooked, related to predicted relative intensities of the different monomeric electronic transitions (in this case the intensity of L_b transitions in one-photon absorption). Scaling the transition electric dipole moment of L_b , so to match the L_b/L_a intensity ratio in the monomer improves the agreement with experiments. Despite the attractiveness of these trivial adjustments, it is important to highlight that any correction of the parameters used in FrDEx requires detailed

scrutiny and that the procedure we have followed here cannot be considered of general applicability. In fact, shifting the energy of only the LE states clearly impacts the interaction between LE and CT states and may lead to a not well-balanced treatment of CT transitions, affecting the accuracy of the spectral shapes in cases where they do play a role. On the other hand, such a computational approach might be used to control possible imbalances in the treatment of LEs and CT states within TDDFT,⁵⁸ although it should be established a well-defined strategy to correct the CT energy, such as the Δ SCF-like approach used in Li et al.⁴⁵

Another potential source of error is that the transition electric dipole moment of a given transition depends on its description in terms of involved molecular orbitals, and it is thus related to all the terms (energy and couplings) of the FrDEx Hamiltonian. Finally, when comparing the computed spectra with the experimental ones, it is important to remember that conformational averaging could affect the spectra²⁷ and that the shape of the high-energy region of the spectra is surely affected by possible limitations in the number of electronic transitions included in the FrDEx procedure.

Overall, this study provides encouraging indications on the use of our procedure to compute the ECD spectra of challenging systems such as GQs. PCM/TD-DFT spectra are in fair agreement with the experiments, and FrDEx spectra are much closer to the reference QM ones than those obtained with simpler excitonic Hamiltonians. The accuracy of FrDEx Hamiltonian can be easily tuned, increasing the number of bases considered in the fragment diabatisation procedure,²⁶ but this would also increase its computational cost.

As a consequence, when the inclusion of conformational effects is important and, thus, the calculation of the ECD spectra on a representative sample of the structure is necessary, it could be useful to integrate the three different approaches. For example, one single full QM for a representative structure (e.g., the experimentally determined one), complemented by many FrDEx calculations and, if it is necessary to map a global conformational rearrangement, by a larger number of “standard” excitonic computations.

ACKNOWLEDGMENTS

The authors thank the CNR program “Progetti di Ricerca @cnr”, project UCATG4. FS thanks financial support from ICSC-Centro Nazionale di Ricerca in High Performance Computing, Big Data, and Quantum Computing, funded by the European Union-NextGenerationEU-PNRR, Missione 4 Componente 2 Investimento 1.4. RI thanks financial support from CN3, National Center for Gene Therapy and Drugs based on RNA technology,

funded by the European Union-NextGenerationEU-PNRR. Open Access Funding provided by Consiglio Nazionale delle Ricerche within the CRUI-CARE Agreement.

DATA AVAILABILITY STATEMENT

Data are available from the authors upon request.

ORCID

James A. Green  <https://orcid.org/0000-0002-5036-3104>

Fabrizio Santoro  <https://orcid.org/0000-0003-4402-2685>

REFERENCES

- Berova N, Nakanishi K, Woody R. *Circular Dichroism. Principles and Applications*. 2nd ed.: Wiley; 2000.
- del Villar-Guerra R, Trent JO, Chaires JB. G-quadruplex secondary structure obtained from circular dichroism spectroscopy. *Angew Chem, Int Ed*. 2018;57:7171-7175.
- Gray DM, Wen J-D, Gray CW, et al. Measured and calculated cd spectra of g-quartets stacked with the same or opposite polarities. *Chirality*. 2008;20(3-4):431-440. <https://doi.org/10.1002/chir.20455>
- Hache F, Changenet P. Multiscale conformational dynamics probed by time-resolved circular dichroism from seconds to picoseconds. *Chirality*. 2021;33(11):747-757. <https://doi.org/10.1002/chir.23359>
- Kypr J, Kejnovská I, Renčíuk D, Vorlíčková M. Circular dichroism and conformational polymorphism of DNA. *Nucleic Acids Res*. 2009;37(6):1713-1725. <https://doi.org/10.1093/nar/gkp026>
- Randazzo A, Spada GP, da Silva MW. Circular dichroism of quadruplex structures; 2013:67-86. https://doi.org/10.1007/128_2012_331
- Vorlíčková M, Kejnovská I, Bednářová K, Renčíuk D, Kypr J. Circular dichroism spectroscopy of DNA: from duplexes to quadruplexes. *Chirality*. 2012;24(9):691-698. <https://doi.org/10.1002/chir.22064>
- Vorlíčková M, Kejnovská I, Sagi J, et al. Circular dichroism and guanine quadruplexes. *Methods*. 2012;57(1):64-75. <http://www.sciencedirect.com/science/article/pii/S1046202312000679>
- Chen X-C, Chen S-B, Dai J, et al. Tracking the dynamic folding and unfolding of RNA G-quadruplexes in live cells. *Angewandte Chemie Int Edition*. 2018;57(17):4702-4706. <https://doi.org/10.1002/anie.201801999>
- Di Antonio M, Ponjavic A, Radzevicius A, et al. Single-molecule visualization of DNA G-quadruplex formation in live cells. *Nat Chem*. 2020;12:832.
- Rhodes D, Lipps HJ. G-quadruplexes and their regulatory roles in biology. *Nucleic Acids Res*. 2015;43(18):8627-8637. <https://doi.org/10.1093/nar/gkv862>
- Carvalho J, Mergny J-L, Salgado GF, Queiroz JA, Cruz C. G-quadruplex, friend or foe: the role of the G-quartet in anticancer strategies. *Trends Mol Med*. 2020;26:848-861.
- Kosiol N, Juranek S, Brossart P, Heine A, Paeschke K. G-quadruplexes: a promising target for cancer therapy. *Mol Cancer*. 2021;20:40.
- Varshney D, Spiegel J, Zyner K, Tannahill D, Balasubramanian S. The regulation and functions of dna and rna G-quadruplexes. *Nat Rev Mol Cell Biol*. 2020;21:459-474.

15. Neidle S, Balasubramanian S, eds. *Quadruplex Nucleic Acids*, RSC Biomolecular Sciences: The Royal Society of Chemistry; 2006. <https://doi.org/10.1039/9781847555298>
16. Yang DS, Lin C, eds. *G-quadruplex Nucleic Acids*, Methods in Molecular Biology: Humana, New York, NY; 2019.
17. Karsisiotis AI, Hessari NM, Novellino E, Spada GP, Randazzo A, Webba da Silva M. Topological characterization of nucleic acid G-quadruplexes by UV absorption and circular dichroism. *Angewandte Chemie Int Edition*. 2011;50(45):10645-10648. <https://doi.org/10.1002/anie.201105193>
18. Masiero S, Trotta R, Pieraccini S, et al. A non-empirical chromophoric interpretation of CD spectra of dna G-quadruplex structures. *Org Biomol Chem*. 2010;8:2683-2692. <https://doi.org/10.1039/C003428B>
19. Improta R. Quantum mechanical calculations unveil the structure and properties of the absorbing and emitting excited electronic states of guanine quadruplex. *Chem-Eur J*. 2014;20:8106-8115.
20. Martínez-Fernández L, Banyasz A, Markovitsi D, Improta R. Topology controls the electronic absorption and delocalization of electron holes in guanine quadruplexes. *Chem-Eur J*. 2018;24(57):15185-15189. <https://doi.org/10.1002/chem.201803222>
21. Martínez-Fernández L, Changenet P, Banyasz A, Gustavsson T, Markovitsi D, Improta R. Comprehensive study of guanine excited state relaxation and photoreactivity in G-quadruplexes. *J Phys Chem Lett*. 2019;10(21):6873-6877. <https://doi.org/10.1021/acs.jpcclett.9b02740>
22. Martínez-Fernández L, Esposito L, Improta R. Studying the excited electronic states of guanine rich dna quadruplexes by quantum mechanical methods: main achievements and perspectives. *Photochem Photobiol Sci*. 2020;19:436-44. <https://doi.org/10.1039/D0PP00065E>
23. Gattuso H, Spinello A, Terenzi A, Assfeld X, Barone G, Monari A. Circular dichroism of dna G-quadruplexes: combining modeling and spectroscopy to unravel complex structures. *J Phys Chem B*. 2016;120(12):3113-3121.
24. Jurinovich S, Cupellini L, Guido CA, Mennucci B. Exat: excitonic analysis tool. *J Comput Chem*. 2018;39(5):279-286. <https://doi.org/10.1002/jcc.25118>
25. Loco D, Jurinovich S, Bari LD, Mennucci B. A fast but accurate excitonic simulation of the electronic circular dichroism of nucleic acids: how can it be achieved? *Phys Chem Chem Phys*. 2016;18:866-877. <https://doi.org/10.1039/C5CP06341H>
26. Green JA, Asha H, Santoro F, Improta R. Excitonic model for strongly coupled multichromophoric systems: the electronic circular dichroism spectra of guanine quadruplexes as test cases. *J Chem Theory Comput*. 2021;17(1):405-415.
27. Asha H, Green JA, Martínez-Fernández L, Esposito L, Improta R. Electronic circular dichroism spectra of DNA quadruple helices studied by molecular dynamics simulations and excitonic calculations including charge transfer states. *Molecules*. 2021;26(16):4789. <https://www.mdpi.com/1420-3049/26/16/4789>
28. Asha H, Green JA, Esposito L, Martínez Fernández L, Santoro F, Improta R. Effect of the thermal fluctuations of the photophysics of GC and CG dna steps: a computational dynamical study. *J Phys Chem B*. 2022;126(50):10608-10621. <https://doi.org/10.1021/acs.jpcc.2c05688>
29. Marathias VM, Wang KY, Kumar S, Pham TQ, Swaminathan S, Bolton PH. Determination of the number and location of the manganese binding sites of DNA quadruplexes in solution by EPR and NMR in the presence and absence of thrombin. *J Molecular Biol*. 1996;260(3):378-394. <https://www.sciencedirect.com/science/article/pii/S0022283696904088>
30. Schultze P, Macaya RF, Feigon J. Three-dimensional solution structure of the thrombin-binding DNA aptamer d (gggtgtgtgtgtgg). *J Molecular Biol*. 1994;235(5):1532-1547. <https://www.sciencedirect.com/science/article/pii/S0022283684711053>
31. Ambrus A, Chen D, Dai J, Jones RA, Yang D. Solution structure of the biologically relevant G-quadruplex element in the human c-Myc promoter. Implications for G-quadruplex stabilization. *Biochemistry*. 2005;44(6):2048-2058, PMID: 15697230. <https://doi.org/10.1021/bi048242p>
32. Phan AT, Kuryavii V, Luu KN, Patel DJ. Structure of two intramolecular G-quadruplexes formed by natural human telomere sequences in k+ solution. *Nucleic Acids Res*. 2007;35(19):6517-6525.
33. Green JA, Yaghoubi Jouybari M, Asha H, Santoro F, Improta R. Fragment diabatisation linear vibronic coupling model for quantum dynamics of multichromophoric systems: population of the charge-transfer state in the photoexcited guanine-cytosine pair. *J Chem Theory Comput*. 2021;17(8):4660-4674. <https://doi.org/10.1021/acs.jctc.1c00416>
34. Dreuw A, Head-Gordon M. Single-reference ab initio methods for the calculation of excited states of large molecules. *Chem Rev*. 2005;105:4009.
35. Zuluaga C, Spata VA, Matsika S. Benchmarking quantum mechanical methods for the description of charge-transfer states in π -stacked nucleobases. *J Chem Theory Comput*. 2021;17(1):376-387, PMID: 33346637. <https://doi.org/10.1021/acs.jctc.0c00973>
36. Zhao Y, Truhlar DG. Density functionals with broad applicability in chemistry. *Accounts Chem Res*. 2008;41(2):157-167. <https://doi.org/10.1021/ar700111a>
37. Improta R, Santoro F, Blancafort L. Quantum mechanical studies on the photophysics and the photochemistry of nucleic acids and nucleobases. *Chem Rev*. 2016;116:3540-3593.
38. Martínez Fernández L, Santoro F, Improta R. Nucleic acids as a playground for the computational study of the photophysics and photochemistry of multichromophore assemblies. *Accounts Chem Res*. 2022;55(15):2077-2087, PMID: 35833758. <https://doi.org/10.1021/acs.accounts.2c00256>
39. Tomasi J, Mennucci B, Cammi R. Quantum mechanical continuum solvation models. *Chem Rev*. 2005;105:2999-3094.
40. Frisch MJ, Trucks GW, Schlegel HB, et al. Gaussian 16 Revision C.01. Gaussian Inc. Wallingford CT; 2016.
41. Santoro F, Green AJ. Overdia1.0, a Fortran 90 code for parameterization of model Hamiltonians based on a maximum-overlap diabatisation, 2022. available free of charge at; <http://www.iccom.cnr.it/overdia-en/>
42. Iozzi MF, Mennucci B, Tomasi J, Cammi R. Excitation energy transfer (EET) between molecules in condensed matter: a novel application of the polarizable continuum model (PCM). *J Chem Phys*. 2004;120(15):7029-7040.
43. Cupellini L, Caprasecca S, Guido CA, Müh F, Renger T, Mennucci B. Coupling to charge transfer states is the key to

- modulate the optical bands for efficient light harvesting in purple bacteria. *J Phys Chem Lett.* 2018;9(23):6892-6899. <https://doi.org/10.1021/acs.jpcclett.8b03233>
44. Jurinovich S, Pescitelli G, Di Bari L, Mennucci B. A TDDFT/MMPOL/PCM model for the simulation of exciton-coupled circular dichroism spectra. *Phys Chem Chem Phys.* 2014;16:16407-16418. <https://doi.org/10.1039/C3CP55428G>
 45. Li X, Parrish RM, Liu F, Kokkila Schumacher SIL, Martínez TJ. An ab initio exciton model including charge-transfer excited states. *J Chem Theory Comput.* 2017;13(8):3493-3504. <https://doi.org/10.1021/acs.jctc.7b00171>
 46. Nottoli M, Jurinovich S, Cupellini L, Gardiner AT, Cogdell R, Mennucci B. The role of charge-transfer states in the spectral tuning of antenna complexes of purple bacteria. *Photosynthesis Res.* 2018;137(2):215-226. <https://doi.org/10.1007/s11120-018-0492-1>
 47. Avila Ferrer FJ, Cerezo J, Stendardo E, Improta R, Santoro F. Insights for an accurate comparison of computational data to experimental absorption and emission spectra: beyond the vertical transition approximation. *J Chem Theory Comput.* 2013;9(4):2072-2082. <https://doi.org/10.1021/ct301107m>
 48. Green JA, Jouybari MY, Aranda D, Improta R, Santoro F. Non-adiabatic absorption spectra and ultrafast dynamics of DNA and RNA photoexcited nucleobases. *Molecules.* 2021;26(6):1743. <https://www.mdpi.com/1420-3049/26/6/1743>
 49. Marathias VM, Bolton PH. Structures of the potassium-saturated, 2:1, and intermediate, 1:1, forms of a quadruplex DNA. *Nucleic Acids Res.* 2000;28(9):1969-1977. <https://doi.org/10.1093/nar/28.9.1969>
 50. Karunakaran V, Kleinermanns K, Improta R, Kovalenko SA. Photoinduced dynamics of guanosine monophosphate in water from broad-band transient absorption spectroscopy and quantum-chemical calculations. *J Am Chem Soc.* 2009;131(16):5839-5850. <https://doi.org/10.1021/ja810092k>
 51. Wierstra I, Alves J. The c-Myc promoter: still mystery and challenge. *Adv Cancer Res.* 2008;99:113-333. <https://www.sciencedirect.com/science/article/pii/S0065230X07990041>
 52. Bhattacharyya D, Mirihana Arachchilage G, Basu S. Metal cations in g-quadruplex folding and stability. *Front Chemist.* 2016;4:38. <https://www.frontiersin.org/articles/10.3389/fchem.2016.00038>
 53. Phillips K, Dauter Z, Murchie AIH, Lilley DMJ, Luisi B. The crystal structure of a parallel-stranded guanine tetraplex at 0.95 Å resolution edited by R.Huber. *J Molecular Biol.* 1997;273(1):171-182. <https://www.sciencedirect.com/science/article/pii/S0022283697912924>
 54. Asha H, Stadlbauer P, Martínez-Fernández L, et al. Early steps of oxidative damage in dna quadruplexes are position-dependent: quantum mechanical and molecular dynamics analysis of human telomeric sequence containing ionized guanine. *Int J Biol Macromol.* 2022;194:882-894. <https://www.sciencedirect.com/science/article/pii/S0141813021025484>
 55. Cang X, Sponer J, Cheatham TE. Insight into G-DNA structural polymorphism and folding from sequence and loop connectivity through free energy analysis. *J Am Chem Soc.* 2011;133(36):14270-14279.
 56. Hazel P, Huppert J, Balasubramanian S, Neidle S. Loop-length-dependent folding of G-quadruplexes. *J Am Chem Soc.* 2004;126(50):16405-16415.
 57. Islam B, Stadlbauer P, Krepl M, Havrila M, Haider S, Sponer J. Structural dynamics of lateral and diagonal loops of human telomeric G-quadruplexes in extended MD simulations. *J Chem Theory Comput.* 2018;14(10):5011-5026. <https://doi.org/10.1021/acs.jctc.8b00543>
 58. Dreuw A, Head-Gordon M. Failure of time-dependent density functional theory for long-range charge-transfer excited states: the zincbacteriochlorin-bacteriochlorin and bacteriochlorophyll-spheroidene complexes. *J Am Chem Soc.* 2004;126(12):4007-4016. <https://doi.org/10.1021/ja039556n>, PMID: 15038755.

SUPPORTING INFORMATION

Additional supporting information can be found online in the Supporting Information section at the end of this article.

How to cite this article: Asha H, Green JA, Esposito L, Santoro F, Improta R. Computing the electronic circular dichroism spectrum of DNA quadruple helices of different topology: A critical test for a generalized excitonic model based on a fragment diabatisation. *Chirality.* 2023;35(5):298-310. doi:10.1002/chir.23540